Response Assessment of ^{68}Ga-DOTA-E-[c(RGDfK)]^2 PET/CT in Lung Adenocarcinoma Patients Treated with Nintedanib Plus Docetaxel

Oscar Arrieta[1], Francisco O. Garcia-Perez[2], David Michel-Tello[1], Laura-Alejandra Ramírez-Tirado[1], Quetzali Pitalua-Cortes[2], Graciela Cruz-Rico[3], Eleazar-Omar Macedo-Pérez[1], Andrés F. Cardona[4,5], and Jaime de la Garza-Salazar[1]

[1]Thoracic Oncology Unit, Instituto Nacional de Cancerología, Mexico City, Mexico; [2]Department of Nuclear Medicine and Molecular Imagenology, Instituto Nacional de Cancerología, Mexico City, Mexico; [3]Laboratory of Personalized Medicine, Instituto Nacional de Cancerología, Mexico City, Mexico; [4]Clinical and Translational Oncology Group, Clínica del Country, Bogotá, Colombia; and [5]Foundation for Clinical and Applied Cancer Research, Bogotá, Colombia

Nintedanib is an oral angiokinase inhibitor used as second-line treatment for non–small cell lung cancer. New radiotracers, such as ^{68}Ga-DOTA-E-[c(RGDfK)]^2, that target $\alpha_v\beta_3$ integrin might have an impact as a noninvasive method for assessing angiogenesis inhibitors. **Methods:** From July 2011 through October 2015, 38 patients received second-line nintedanib plus docetaxel. All patients underwent PET/CT with ^{68}Ga-DOTA-E-[c(RGDfK)]^2 radiotracer and blood-sample tests to quantify angiogenesis factors (fibroblast growth factor, vascular endothelial growth factor, and platelet-derived growth factor AB) before and after completing 2 therapy cycles. **Results:** Of the 38 patients, 31 had available baseline and follow-up PET/CT. Baseline lung tumor volume addressed with ^{68}Ga-DOTA-E-[c(RGDfK)]^2 PET/CT correlated with serum vascular endothelial growth factor levels, whereas baseline lung/liver SUV_{max} index correlated with platelet-derived growth factor AB. After treatment, the overall response rate and disease control rate were 7.9% and 47.3%, respectively. A greater decrease in lung tumor volume (−37.2% vs. –27.6%) was associated with a better disease control rate in patients ($P = 0.005$). Median progression-free survival was 3.7 mo. Nonsmokers and patients with a higher baseline lung tumor volume were more likely to have a higher progression-free survival (6.4 vs. 3.74 [$P = 0.023$] and 6.4 vs. 2.1 [$P = 0.003$], respectively). Overall survival was not reached. Patients with a greater decrease in lung SUV_{max} (not reached vs. 7.1 mo; $P = 0.016$) and a greater decrease in the lung/spleen SUV_{max} index (not reached vs. 7.1; $P = 0.043$) were more likely to have a longer overall survival. **Conclusion:** ^{68}Ga-DOTA-E-[c(RGDfK)]^2 PET/CT is a potentially useful tool for assessing responses to angiogenesis inhibitors. Further analysis and novel studies are warranted to identify patients who might benefit from this therapy.

Key Words: adenocarcinoma; nintedanib/docetaxel; ^{68}Ga-DOTA-E-[c(RGDfK)]^2; angiogenesis; $\alpha_v\beta_3$ integrin

J Nucl Med 2018; 59:403–409
DOI: 10.2967/jnumed.117.192393

Lung cancer is the leading cause of cancer death worldwide (*1*). Most patients are diagnosed with advanced disease, and most patients treated with first-line platinum-based chemotherapy will experience disease progression after 3–7 mo and require second-line therapy (*2*). Tumors grow by inducing endothelial proliferation to increase existing blood vessels in order to supply the tumor with oxygen and nutrients. Antiangiogenic tyrosine kinase inhibitors have demonstrated a cytostatic effect on tumor cells by slowing growth and preventing development of distant metastases. Nintedanib, an oral angiokinase inhibitor, targets the proangiogenic pathways mediated by vascular endothelial growth factor (VEGF) receptors 1–3, fibroblast growth factor receptor, and platelet-derived growth factor receptors α and β (*3,4*). Hypoxia is the most potent stimulus for their production by activating hypoxia-inducible factor 1α, which upregulates proangiogenic factors, resulting in rapid tumor growth (*5*). VEGF is the most studied and influential proangiogenic factor in the tumoral angiogenic process. Targeting VEGF has become relevant because of its potential for use of new drugs (*6*). Preclinical studies with nintedanib reported sustained blockade of VEGF receptor 2 in vitro and tumor growth arrest (*3*). In phase 1 and 2 clinical trials, nintedanib showed a manageable safety profile and antitumor activity in patients with solid tumors, including non–small cell lung cancer (NSCLC) (*4,7*). The LUME-Lung 1 study demonstrated that patients with adenocarcinoma histology experienced significant improvement in median overall survival (OS) and progression-free survival (PFS) with nintedanib plus docetaxel versus docetaxel alone (*7,8*). Importantly, the subgroup of patients who experienced progression within 9 mo after starting first-line therapy had a significantly longer OS, with a 3-mo increase.

Integrins play a major role in adhesion of cells to extracellular matrix proteins. They are also responsible for regulating removal from the cell cycle and cell migration (*9*). The $\alpha_v\beta_3$ integrin is a transmembrane protein constituting 2 subunits, α and β, and is generally expressed on mature endothelial and epithelial cells, as well as on tumor cells. It favors growth of several angiogenesis-dependent tumors (*10*). The $\alpha_v\beta_3$ integrin can bind to the arginine-glycine-aspartic acid (RGD) amino acid sequence present in extracellular matrix proteins, such as vitronectin, fibrinogen, and laminin (*11*). Because of this characteristic, $\alpha_v\beta_3$ integrin has been identified as a molecular target for noninvasive monitoring of

Received Feb. 28, 2017; revision accepted Jul. 13, 2017.
For correspondence or reprints contact: Oscar Arrieta, Instituto Nacional de Cancerología (INCan), San Fernando #22, Seccion XVI, Tlalpan, Mexico City, Mexico, CP 14080.
E-mail: ogar@unam.mx
Published online Aug. 17, 2017.

malignant cells and treatment response assessment (*12,13*). Furthermore, Zannetti et al., using in vivo murine models, have shown that this peptide does not exhibit a cross-reaction with $\alpha_v\beta_5$, which confers high selectivity in nuclear imaging (*14*). Recently, significant progress has been made in the development of new imaging techniques, including ^{15}O-labeled radiotracers such as ^{15}O water and C^{15}O, which have been used to quantify tumor perfusion that might be related to angiogenesis. In parallel, $\alpha_v\beta_3$-targeting radiotracers for the visualization of $\alpha_v\beta_3$ expression in tumors by PET/CT have been synthesized, resulting in the use of the generator-produced radionuclide ^{68}Ga-DOTA-E-[c(RGDfK)]^2 (*10,13*). The application of ^{68}Ga-DOTA-E-[c(RGDfK)]^2–labeled peptides has attracted interest in cancer imaging because of their physical characteristics along with improved tumor targeting (*15,16*).

Antiangiogenic therapy is a promising treatment for malignancies, including lung cancer. Because these are designed to inhibit tumor growth and dissemination instead of causing direct cytotoxicity, they cannot cause tumors to shrink rapidly in the short term; evaluation of response by CT or ^{18}F-FDG PET/CT is therefore difficult (*17*). However, the ^{68}Ga-DOTA-E-[c(RGDfK)]^2 peptide is a suitable ligand for the noninvasive visualization of $\alpha_v\beta_3$ expression in vivo that can provide information on molecular processes such as angiogenesis and its correlation with chemotherapy response and prognosis (*10,13,15*). In the current study, we tested the ability of PET/CT with the radiotracer ^{68}Ga-DOTA-E-[c(RGDfK)]^2 to assess therapeutic responses to treatment with nintedanib plus docetaxel in lung adenocarcinoma. Furthermore, we evaluated the prognosis as determined by survival.

MATERIALS AND METHODS

Patients

This study was performed at the Instituto Nacional de Cancerología in Mexico City. All patients were adults (>18 y old) who had histologically confirmed stage IIIB or IV lung adenocarcinoma failing to respond to platinum-based first-line chemotherapy, an Eastern Cooperative Oncology Group performance status of less than 2, and measurable disease according to RESIST (version 1.1). We excluded patients who had active brain metastases, received previous docetaxel, or had a recent history (<3 mo) of clinically significant hemoptysis or a major thrombotic or clinically relevant major bleeding event in the past 6 mo. All patients provided written informed consent. The study complied with the protocol and with the Declaration of Helsinki. The protocol was approved by an independent local ethics committee (015/007/ICI) (CEI/889/15).

Treatment Regimen

The patients received docetaxel, 75 mg/m^2, on day 1 plus nintedanib, 200 mg twice daily orally, on days 2–21, every 3 wk. Four cycles were given in combination, and then nintedanib was given alone as maintenance therapy. Nintedanib and docetaxel were provided by Boehringer Ingelheim as part of the Compassionate Use Program for nintedanib. Treatment was continued until disease progression or unacceptable toxicity. All patients were assessed for toxicities before starting each cycle according to the Common Terminology Criteria for Adverse Events (version 4.0).

Imaging

Before and after 2 cycles of treatment, all patients underwent ^{68}Ga-DOTA-E-[c(RGDfK)]^2 PET/CT using an mCT Excel 20 PET/CT scanner (Siemens) consisting of a bismuth orthosilicate full scanner and a 20-detector-row CT scanner. Whole-body CT was performed 40–50 min after injection of 188.7 MBq of ^{68}Ga-RGD (±1.2), and transmission data were acquired using low-dose CT (120 kV, automated from 100 to 130 mA, a 512 × 512 matrix, a 50-cm field of view, a 3.75-mm slice thickness, and a 0.8-s rotation time), extending from the base of the skull to the proximal thighs. After the CT acquisition, a whole-body PET scan was acquired in 3 dimensions (matrix, 168 × 168). For each bed position (16.2 cm; overlapping scale, 4.2 cm), we used a 3-min acquisition time with a 15.5-cm field of view. The emission data were corrected for randoms, scatter, and decay. Reconstruction was conducted with an ordered-subset expectation maximization algorithm with 3 iterations and 12 subsets, Gauss-filtered to a transaxial resolution of 6 mm in full width at half maximum. Attenuation was corrected using low-dose nonenhanced CT. A workstation (Multimodality Workplace; Siemens) providing multiplanar reformatted images was used for image display and analysis. The median tumoral volume and the SUV_{max} of whole-body tumors were measured with the isocontour tool of the TrueD Syngo software (Siemens) using a threshold of 20% of the SUV_{max}, with manual adjustment.

Radiopharmaceutical Preparation

^{68}Ga-DOTA-E-[c(RGDfK)]^2 was synthesized according to the method described by López-Rodriguez et al. (*16*)

PET/CT Interpretation Criteria

^{68}Ga-DOTA-E-[c(RGDfK)]^2 PET/CT was performed before the start of treatment and again after 2 cycles of treatment. Negative PET/CT results were defined as tracer confined to normal-uptake organs (spleen, urinary bladder, liver) and no other sites with uptake (*16,18*). Positive results (progressive disease) were defined as at least one focus of abnormally intense uptake, characterized by visual inspection or SUV_{max} measurements. PET/CT images were visually analyzed by experienced nuclear medicine physicians.

Determination of Serum Angiogenesis Factors

Two serum samples were collected at baseline and after 2 therapy cycles. Serum levels were determined using enzyme-linked immunosorbent assays, which were performed using Quantikine human fibroblast growth factor, VEGF, and platelet-derived growth factor AB immunoassay kits (DFB50, DHD00C, and DVE00, respectively; R&D Systems). All assays were performed in duplicate.

Outcomes

The primary endpoint was disease control rate (DCR) addressed by ^{68}Ga-DOTA-E-[c(RGDfK)]^2 PET/CT. Secondary endpoints included overall response rate, PFS, OS, and toxicity profile. DCR was defined as the percentage of patients with advanced or metastatic NSCLC who achieved a complete response, a partial response, or stable disease after treatment with nintedanib plus docetaxel. The overall response rate was defined as the percentage of patients with advanced or metastatic NSCLC who achieved a complete and partial response to nintedanib plus docetaxel. PFS was defined as the time from the start of treatment with nintedanib until disease progression or death, and OS was defined as the time from the start of treatment with nintedanib until the last follow-up or death.

Statistical Analysis

Continuous variables were summarized as mean with SD, categoric variables as frequency and percentage. The χ^2 or Fisher exact test was used to assess the significance of differences among categoric variables. Patients were stratified by DCR, and the median values for the PET/CT parameters were addressed by paired *t* tests considering baseline and follow-up values. The percentage change (%Δ) was also calculated for baseline and follow-up PET/CT parameters.

Median OS and PFS were estimated using the Kaplan–Meier method. The median follow-up was 8.8 mo (range, 6.2–11.4 mo).

The log-rank test was used for comparisons among subgroups. A multivariate Cox–proportional hazard model was used. All variables were dichotomized for the survival analyses. Statistical significance was determined as a P value of 0.05 or less using a 2-tailed test. SPSS software (version 21; SPSS Inc.) was used for all statistical analysis.

RESULTS

Study Design

Forty-six patients were assessed for eligibility, and 8 were excluded. The remaining 38 patients underwent PET/CT with ^{68}Ga-DOTA-E-[c(RGDfK)]^2. Five patients did not complete therapy because of unacceptable toxicity ($n = 1$) or early disease progression ($n = 4$). Therefore, at the final follow-up, there were 33 patients, but 2 were excluded from the final analysis because of missing data (Fig. 1).

Characteristics of Patients

Among the 38 patients, 16% (6/38) had diabetes and 29% (11/38) had systemic hypertension at enrollment. Most patients had a good Eastern Cooperative Oncology Group performance status (<2) (97%; 37/38). The most common lung adenocarcinoma histologic subtypes were acinar (21%) and papillary (16%) The first-line overall response rate and DCR were 47% (18/38) and 74% (28/38), respectively (Supplemental Table 1; supplemental materials are available at http://jnm.snmjournals.org).

Treatment Characteristics

The overall response rate and DCR for nintedanib plus docetaxel were 8% (3/38) and 47% (18/38), respectively. When we analyzed the patients stratified by DCR with nintedanib, we did not find differences among them by sex, median age, exposure to tobacco, diabetes, number of metastases, histologic grade differentiation, or median carcinoembryonic antigen. The presence of systemic hypertension was associated with a better DCR (77.8 vs. 22.2), although the difference was not statistically significant ($P = 0.125$) (Supplemental Table 2).

Adverse Events

Only 34% (13/38) of patients experienced severe adverse events requiring hospitalization. The most frequent adverse events were anemia (68%), nausea (66%), leukopenia (63%), and dyspnea (61%). The most common severe adverse events (graded ≥ 3) were neutropenia (21%), dyspnea (18%), leukopenia (16%), and asthenia (13%).

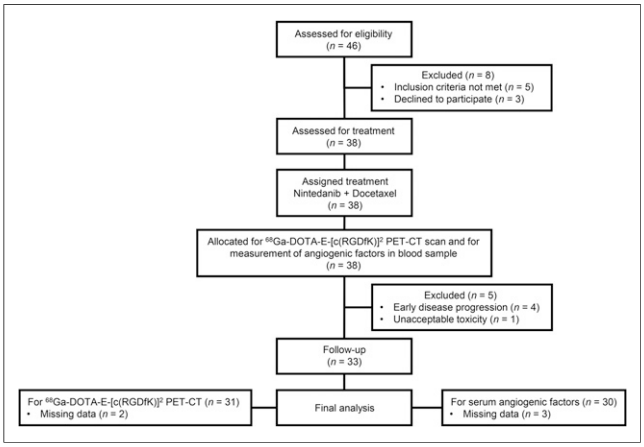

FIGURE 1. Flow diagram of patients included in analysis.

Assessment of ^{68}Ga-DOTA-E-[c(RGDfK)]^2 PET/CT Radiotracer

Figure 2 shows the therapeutic response to antiangiogenic therapy. The ^{68}Ga-DOTA-E-[c(RGDfK)]^2 PET/CT scan before treatment showed intense avidity for the radiotracer in the right lung lesion and in the ipsilateral and contralateral mediastinal lymph nodes, with an SUV_{max} of 7.6. The follow-up PET/CT scan showed a significant reduction of avidity in the lung lesion and lymph nodes, with a decreased SUV_{max} of 3.5 (Fig. 2).

Baseline, Follow-up, and %Δ in ^{68}Ga-DOTA-E-[c(RGDfK)]^2 PET/CT Parameters and Angiogenic Factors

The assessment parameters for ^{68}Ga-DOTA-E-[c(RGDfK)]^2 PET/CT are shown in Table 1. After treatment with nintedanib plus docetaxel, the parameters that showed a statistically significant reduction were lung/spleen SUV_{max} index (%Δ, −13%; $P = 0.022$) and lung tumor volume (%Δ, −38%; $P = 0.002$). By contrast, the follow-up parameters that showed an increase after the antiangiogenic therapy were fibroblast growth factor (%Δ, 125%; $P = 0.030$) and platelet-derived growth factor AB (%Δ, 70%; $P = 0.035$) (Table 1).

^{68}Ga-DOTA-E-[c(RGDfK)]^2 PET/CT Parameters and Therapeutic Response to Nintedanib

PET/CT parameters stratified according to DCR showed that patients who did not achieve disease control had a higher and significant ($P = 0.008$) %Δ reduction (−30%) in lung tumor/spleen SUV_{max} index, compared with patients who achieved disease control (−13%; $P = 0.806$). By contrast, patients who achieved disease control had a higher and significant decrease in lung tumor volume (−37%; $P = 0.005$) than patients who did not achieve disease control (−28%; $P = 0.088$). When we compared %Δ in lung tumor volume as assessed by RESIST with %Δ in baseline lung tumor SUV_{max} as assessed by ^{68}Ga-DOTA-E-[c(RGDfK)]^2 PET/CT, we found that most patients who achieved disease control had a decrease in %Δ in lung tumor SUV_{max} (Fig. 3).

^{68}Ga-DOTA-E-[c(RGDfK)]^2 PET/CT Parameters and Angiogenic Factors

When the relationship between ^{68}Ga-DOTA-E-[c(RGDfK)]^2 PET/CT parameters and angiogenic factors (fibroblast growth factor, VEGF, platelet-derived growth factor AB) was analyzed, a positive correlation was found between baseline lung tumor/liver SUV_{max} index and baseline platelet-derived growth factor AB ($r^2 = 0.418$; $P = 0.030$). Likewise, baseline lung tumor volume and baseline VEGF showed a positive correlation with each other ($r^2 = 0.574$; $P = 0.003$).

Factors Associated with PFS and OS

The median PFS was 3.7 mo. A greater baseline lung tumor volume (≥19.1 vs. < 19.1) was associated with a higher PFS (6.4 vs. 2.1; $P = 0.007$). (Fig. 4). In the multivariate analysis, systemic hypertension was associated with longer PFS (hazard ratio, 0.2; 95% confidence interval, 0.1–0.80; $P = 0.021$).

OS was not reached. A higher %Δ in lung tumor SUV_{max} (≥−19% vs. <−19%) was associated with a higher OS (not reached vs. 7.1; $P = 0.016$). Patients with a higher baseline lung tumor/spleen SUV_{max} index (≥0.8 vs. <0.8) were more likely to have a longer OS (not reached vs. 4.6 mo; $P = 0.022$). Moreover, a higher lung tumor/spleen SUV_{max} index (≥−13% vs. <13%) was associated with a higher OS (not reached vs. 7.8; $P = 0.043$)

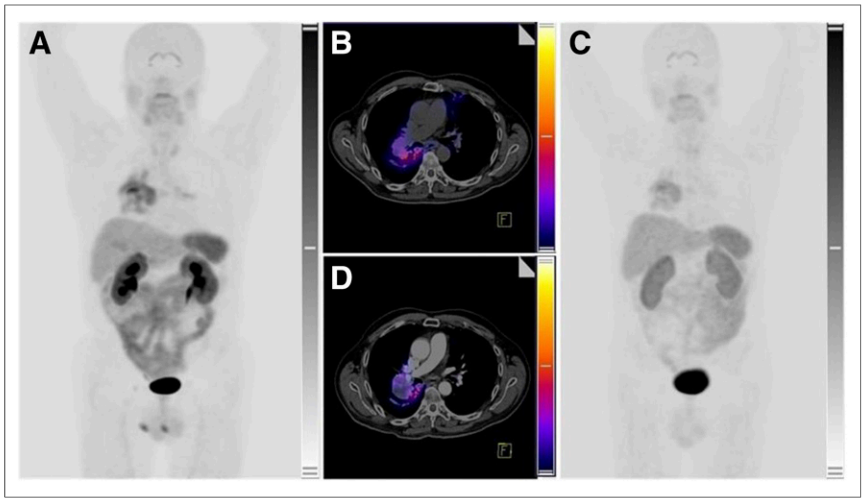

FIGURE 2. A 62-y-old man with lung adenocarcinoma. (A and B) ^{68}Ga-DOTA-E-[c(RGDfk)]^2 PET/CT before treatment with multikinase inhibitors shows intense avidity for radiotracer in right lung lesion and in ipsilateral and contralateral mediastinal lymph nodes. Tumor volume is 178 cm^3, with SUV_{max} of 7.6. (C and D) PET/CT posttherapy images show significant reduction of avidity in lung lesion and lymph nodes, with tumor volume of 56 cm^3 and SUV_{max} of 3.5 (scale, 0–10 SUV-body weight). PFS of this patient was 6 mo.

(Fig. 4). In the multivariate analysis, %Δ in lung tumor SUV_{max} was associated with a worse OS (hazard ratio, 3.1; 95% confidence interval, 1.0–9.8; $P = 0.048$).

DISCUSSION

Targeted therapies have changed treatment for lung cancer patients. Nevertheless, the treatment of most will progress to chemotherapy alone. Antiangiogenic agents have been studied in NSCLC with poor results. Bevacizumab, a monoclonal antibody against serum VEGF, improved prognosis in first-line settings in combination with paclitaxel or pemetrexed (*17,19*). NSCLC patients harboring an EGFR mutation have also shown a better PFS when treated with the combination of a tyrosine kinase inhibitor plus bevacizumab. In the JO25567 trial, erlotinib plus bevacizumab improved PFS versus erlotinib alone (16 vs. 9.7 mo; hazard ratio, 0.054) (*17*).

Phase III studies on second-line therapy, such as the ZODIAC study (vandetanib ± docetaxel), the ZEAL study (vandetanib ± pemetrexed), and the ZEST study (vandetanib vs. erlotinib), have tested the efficacy of antiangiogenics and reported a limited impact on OS for advanced NSCLC patients (*20*).

Despite these results, there are two antiangiogenic agents that show promise for improving OS after progression on first-line therapy: ramucirumab and nintedanib. Nintedanib is a triple-angiokinase inhibitor targeting fibroblast growth factor, platelet-derived growth factor AB, and VEGF; high levels of the last of these confer a poor prognosis in NSCLC (*21*). The LUME-Lung 1 study, a phase III trial, improved survival rates at 1 y (52.7% vs. 44.7%) and 2 y (25.7% vs. 19.1%) in patients with disease refractory to first-line therapy, especially those with adenocarcinoma. This finding sets the base for biomarker correlation analyses and stratified treatment response assessment (*8*).

Potential biomarkers for angiogenesis have been studied, particularly with anti-VEGF antibodies (*22,23*). A phase 2/3 trial with carboplatin and paclitaxel with or without bevacizumab reported that low VEGF levels may predict a better PFS ($P = 0.04$). Therefore, serum VEGF levels could potentially serve as a tool for identifying patients who might benefit from antiangiogenic inhibitors.

The current need for early diagnosis, stratification, and treatment response assessment has led to innovative techniques for nuclear medicine and molecular imaging. Medical imaging has an advantage as a biomarker by being a noninvasive method that

TABLE 1
Baseline, Follow-up, and %Δ in ^{68}Ga-DOTA-E-[c(RGDfK)]^2 PET/CT and Angiogenic Soluble Factors ($n = 31$)

Parameter	Baseline		Follow-up			
	Median	Range	Median	Range	Median %Δ	Wilcoxon *P*
Lung tumor SUV_{max}	4.3	1.3–9.2	3.5	1.8–7.8	−18.6	0.188
Spleen SUV_{max}	5.0	1.6–8.4	5.8	2.4–12.1	16	0.427
Liver SUV_{max}	3.2	1.0–5.5	3.3	1.6–6.5	3.1	0.666
Lung tumor/spleen SUV_{max} index	0.8	0.4–1.6	0.7	0.3–1.3	−12.5	0.022
Lung tumor/liver SUV_{max} index	1.4	0.6–2.3	1.2	0.4–2.8	−14.2	0.057
Lung tumor volume	19.1	0.5–557.1	11.9	0–634.4	−37.7	0.002
FGF (pg/mL)	39.2	3.2–337	88.1	8.1–297.8	124.7	0.030
VEGF (pg/mL)	182.4	1.9–609.2	193.1	23.6–574.4	5.9	0.253
PDGF-AB (pg/mL)	8,655.6	2,136.1–32,150.0	14,700.0	1,681.9–39,038.9	69.8	0.035

FGF = fibroblast growth factor; PDGF-AB = platelet-derived growth factor AB.
Seven patients (18.4%) were excluded because of missing values at follow-up.

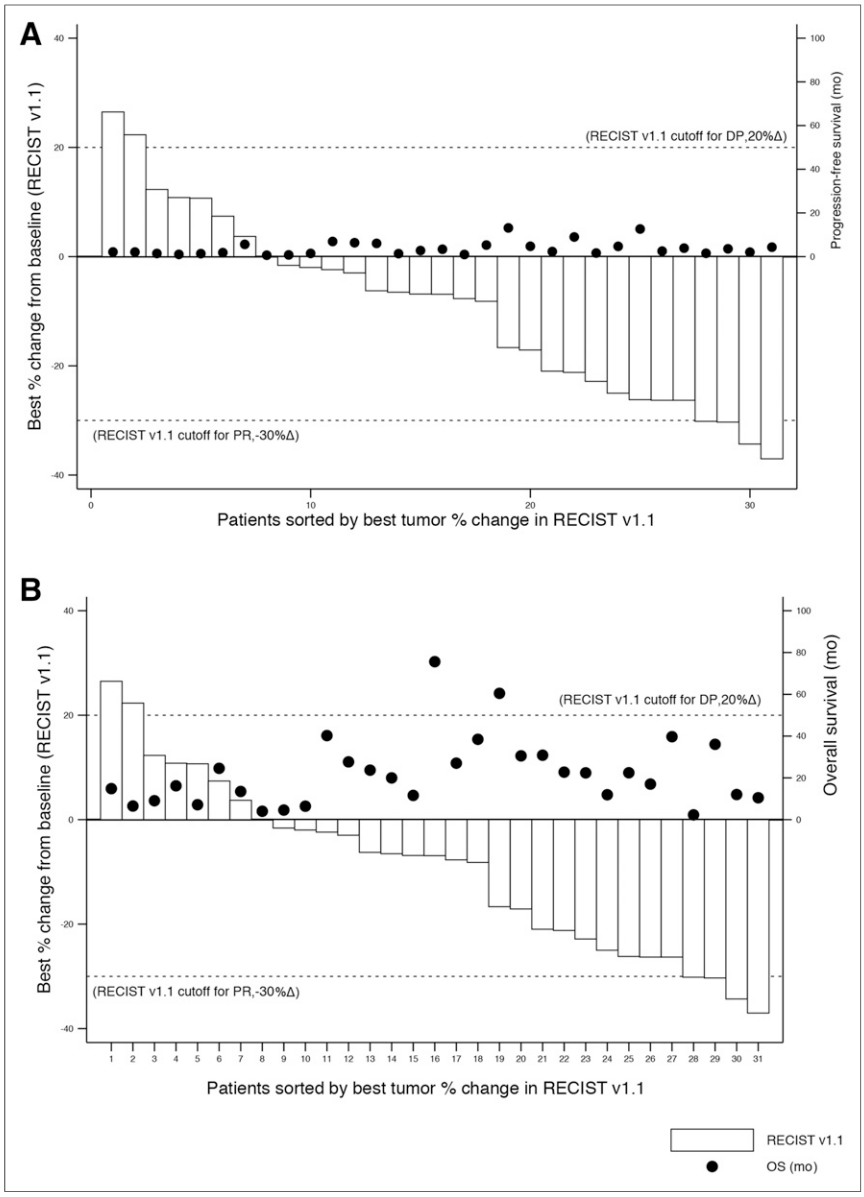

FIGURE 3. Waterfall plots of %Δ in tumoral volume by RECIST (A) and by lung tumor SUV_{max} measured with ^{68}Ga-DOTA-E-[c(RGDfk)]^2 PET/CT (B). PR = partial response.

can provide a variety of information about the tumor (*24*). Integrated PET/CT using ^{18}F-FDG, the most widespread image radiotracer, can visualize tumor viability, tumor anatomy, and the surrounding normal tissues. The reported sensitivity, specificity, and accuracy of ^{18}F-FDG PET/CT are 89%, 94%, and 93%, respectively (*25*). However, it lacks tumor specificity and has poor uptake in tumor-related neovascularization (*18,26*). Thus, new approaches and optimal imaging methods must be established for new drugs, such as antiangiogenic therapies.

An increased expression of $\alpha_v\beta_3$ integrin in tumoral endothelium and tumor cells is associated with invasion and metastasis (*27*). Furthermore, the 2-subunit composition of $\alpha_v\beta_3$ integrin makes it a suitable, although not exclusive, receptor for the RGD sequence in the ^{68}Ga-DOTA-E-[c(RGDfK)]^2 radiotracer. In fact, other integrins (e.g., $\alpha_v\beta_5$, $\alpha_v\beta_6$) are also related to RGD amino acid sequence binding (*28,29*). The $\alpha_v\beta_3$ integrin is targetable by various radiolabeled RGD peptides (*30*). Histologically, RGD peptides target tumor vasculature via RGD-integrin $\alpha_v\beta_3$ interaction, with little extravasation. Therefore, decreased $\alpha_v\beta_3$ integrin expression measured by this imaging method can be associated with proper antiangiogenic blockade (*28*). However, because tumor cells are also known to express several integrins, the overall uptake of an RGD peptide may very well be influenced by the expression of $\alpha_v\beta_3$, or other integrins, on the tumor tissue (*27*).

This study represents, to the best of our knowledge, the first evaluation of the response to nintedanib plus docetaxel in lung adenocarcinoma patients using ^{68}Ga-DOTA-E-[c(RGDfK)]^2 PET/CT as a surrogate biomarker. Our study also develops a prognostic model using dynamic molecular imaging. We demonstrate the relationship that exists between angiogenic metabolic volume and response to the multikinase inhibitor—a relationship that would follow from that between RGD peptide uptake and union to $\alpha_v\beta_3$ integrins. In this second-line study using a targeted agent with chemotherapy, we determined survival rates (OS and PFS), therapy response rates (overall response rate and DCR), and statistical correlations between PET/CT parameters and clinical characteristics.

For the overall response rate and DCR assessment by PET/CT, the results resembled those of the LUME-Lung 1 study, with no precedent of a tyrosine kinase inhibitor in combination with chemotherapy as second-line treatment, the response to which was measured using ^{68}Ga-DOTA-E-[c(RGDfK)]^2 PET/CT. The main parameter used to assess overall response rate was tumor volume, which showed a statistically significant reduction, mainly because of the metabolic decrease in target lesions after 2 cycles of nintedanib plus docetaxel. There were also significant differences in the uptake rate of ^{68}Ga-DOTA-E-[c(RGDfK)]^2 in DCR between responders and nonresponders. Another important finding was that variations in the RECIST measurement and the lung tumor %Δ in SUV_{max} seemed similar, which highlights that this study, one of the first of its class, could achieve the intended regulation for the use of ^{68}Ga-DOTA-E-[c(RGDfK)]^2 PET/CT as a method to monitor disease control for antiangiogenic drugs.

Additionally, when we assessed PFS, a higher baseline lung tumor volume was associated with a longer period until progression, which was consistent with previous results (*16,31,32*). Thus, a higher targetable metabolic area might be associated with a higher tumor burden and therefore with a potentially higher treatment efficacy. We also observed that a higher %Δ in lung tumor SUV_{max} and in lung tumor/spleen SUV_{max} index affected OS but not PFS. These findings suggest a high correlation with

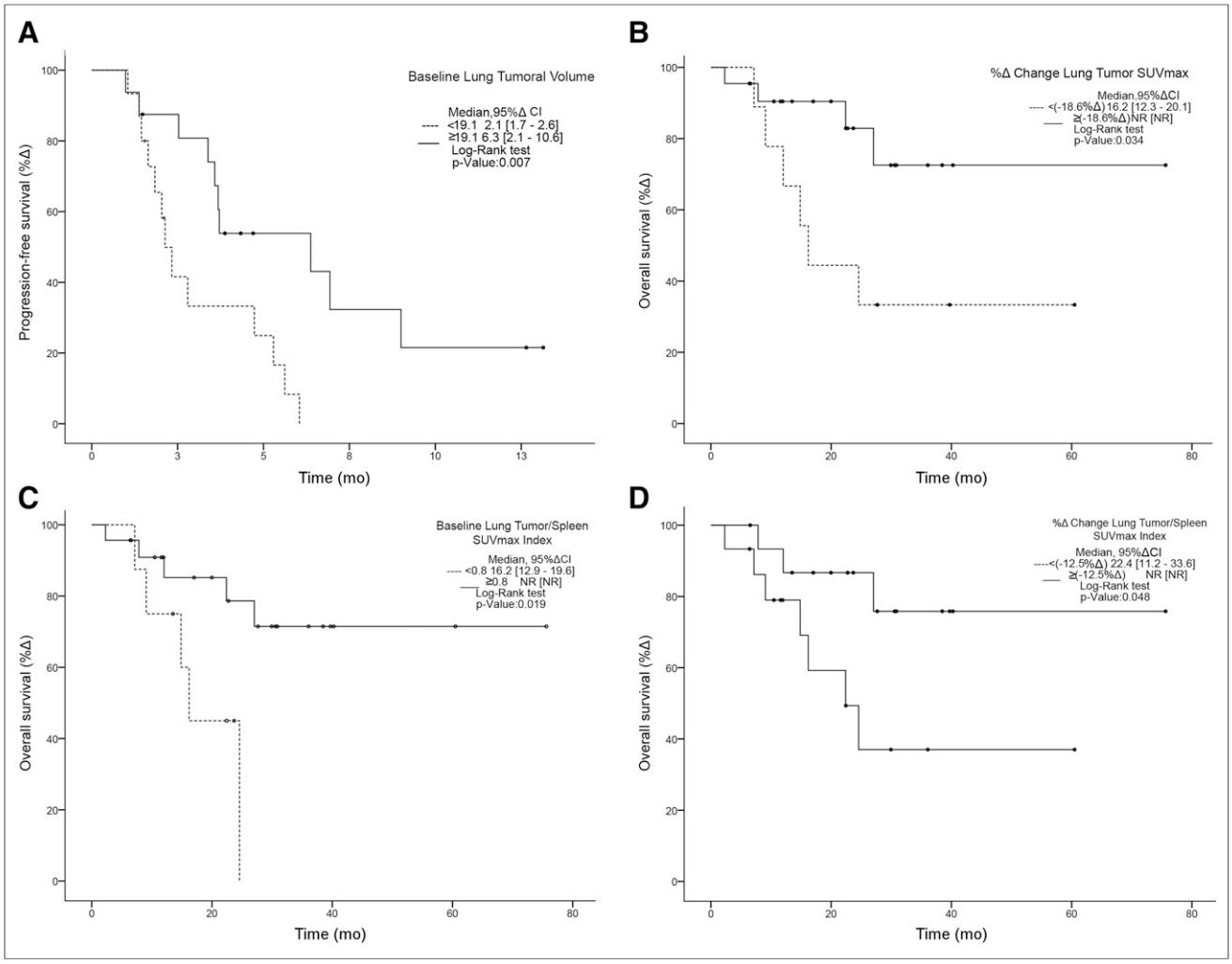

FIGURE 4. Kaplan–Meier curves for significant differences in PFS (A) and OS (B–D). CI = confidence interval; NR = not reached.

therapeutic response to nintedanib. Our observations are consistent with a previous study investigating a ^{68}Ga-labeled pegylated RGD dimer (*28*). Validated by ex vivo immunohistochemistry, the authors found that the RGD radiotracer uptake was significantly reduced after antiangiogenic therapy, reflecting tumor response significantly earlier than is possible with ^{18}F-FDG PET/CT. Contrary results were reported by Rylova et al., who studied ^{68}Ga-NODAGA-RGD for the in vivo monitoring of bevacizumab monotherapy in human squamous cell carcinoma xenografts in mice (*33*). Despite a reduced $\alpha_v\beta_3$ integrin expression under VEGF inhibition, they observed an increased binding of ^{68}Ga-NODAGA-RGD in the investigated A-431 xenografts. Rylova et al. therefore concluded that RGD radiotracer uptake might not reflect changes in $\alpha_v\beta_3$ integrin expression at the molecular level. They hypothesized that bevacizumab may activate $\alpha_v\beta_3$ integrin, causing a higher affinity to ^{68}Ga-NODAGA-RGD and consequently increased radiotracer uptake in vivo (*33*). Assuming a high-affinity state of $\alpha_v\beta_3$ integrin, however, one would expect an increased binding of the primary anti–$\alpha_v\beta_3$ integrin antibody used in the immunohistochemical stainings and consequently false high $\alpha_v\beta_3$ integrin levels. However, in line with our results, the authors found a reduced $\alpha_v\beta_3$ integrin expression in the therapy group. In addition, VEGF is known to indirectly activate $\alpha_v\beta_3$ integrin (*34*).

Our study had limitations, such as sample size and the relatively immature data used for estimating OS. Nonetheless, our study had the advantage of being the first prospective clinical trial assessing therapeutic response with ^{68}Ga-DOTA-E-[c(RGDfK)]^2, which in the future might also become a delivering radiotracer for refractory patients. Additionally, our results showed a high concordance with those of the LUME-1 study, had a larger population-based clinical trial, and highlighted a similar therapeutic response among Caucasian, Asian, and Hispanic patients with adenocarcinoma treated with nintedanib plus docetaxel.

CONCLUSION

^{68}Ga-DOTA-E-[c(RGDfK)]^2 PET/CT is a potentially useful tool for assessing response to angiogenesis inhibitors. The present study may provide the clinical basis for future studies investigating RGD-based hybrid imaging for monitoring therapeutic responses to molecular cancer therapies. RGD-based hybrid imaging may allow for a noninvasive real-time molecular typing of lung adenocarcinoma under antiangiogenic treatment, adding

complementary biomarkers of a therapeutic response to morphology-based and functional tumor response assessments.

DISCLOSURE

No potential conflict of interest relevant to this article was reported.

ACKNOWLEDGMENT

This work was presented as a poster at the 2016 World Conference on Lung Cancer in Vienna, Austria.

REFERENCES

1. Ferlay J, Soerjomataram I, Dikshit R, et al. Cancer incidence and mortality worldwide: sources, methods and major patterns in GLOBOCAN 2012. *Int J Cancer.* 2015;136:E359–E386.
2. Garon EB, Ciuleanu TE, Arrieta O, et al. Ramucirumab plus docetaxel versus placebo plus docetaxel for second-line treatment of stage IV non-small-cell lung cancer after disease progression on platinum-based therapy (REVEL): a multicentre, double-blind, randomised phase 3 trial. *Lancet.* 2014;384:665–673.
3. Hilberg F, Roth GJ, Krssak M, et al. BIBF 1120: triple angiokinase inhibitor with sustained receptor blockade and good antitumor efficacy. *Cancer Res.* 2008; 68:4774–4782.
4. Mross K, Stefanic M, Gmehling D, et al. Phase I study of the angiogenesis inhibitor BIBF 1120 in patients with advanced solid tumors. *Clin Cancer Res.* 2010;16:311–319.
5. Kerbel R, Folkman J. Clinical translation of angiogenesis inhibitors. *Nat Rev Cancer.* 2002;2:727–739.
6. Gutierrez M, Giaccone G. Antiangiogenic therapy in nonsmall cell lung cancer. *Curr Opin Oncol.* 2008;20:176–182.
7. Reck M, Kaiser R, Eschbach C, et al. A phase II double-blind study to investigate efficacy and safety of two doses of the triple angiokinase inhibitor BIBF 1120 in patients with relapsed advanced non-small-cell lung cancer. *Ann Oncol.* 2011; 22:1374–1381.
8. Reck M, Kaiser R, Mellemgaard A, et al. Docetaxel plus nintedanib versus docetaxel plus placebo in patients with previously treated non-small-cell lung cancer (LUME-Lung 1): a phase 3, double-blind, randomised controlled trial. *Lancet Oncol.* 2014;15:143–155.
9. Jin H, Varner J. Integrins: roles in cancer development and as treatment targets. *Br J Cancer.* 2004;90:561–565.
10. García-Figueiras R, Padhani AR, Beer AJ, et al. Imaging of tumor angiogenesis for radiologists—part 1: biological and technical basis. *Curr Probl Diagn Radiol.* 2015;44:407–424.
11. Gasparini G, Brooks PC, Biganzoli E, et al. Vascular integrin $\alpha_v\beta_3$: a new prognostic indicator in breast cancer. *Clin Cancer Res.* 1998;4:2625–2634.
12. Kumar CC. Integrin αvβ3 as a therapeutic target for blocking tumor-induced angiogenesis. *Curr Drug Targets.* 2003;4:123–131.
13. Ruoslahti E, Pierschbacher MD. New perspectives in cell adhesion: RGD and integrins. *Science.* 1987;238:491–497.
14. Zannetti A, Del Vecchio S, Iommelli F, et al. Imaging of $\alpha_v\beta_3$ expression by a bifunctional chimeric RGD peptide not cross-reacting with $\alpha_v\beta_5$. *Clin Cancer Res.* 2009;15:5224–5233.
15. van Hagen PM, Breeman WA, Bernard HF, et al. Evaluation of a radiolabelled cyclic DTPA-RGD analogue for tumour imaging and radionuclide therapy. *Int J Cancer.* 2000;90:186–198.
16. López-Rodriguez V, Galindo-Sarco C, Garcia-Perez FO, Ferro-Flores G, Arrieta O, Avila-Rodriguez MA. PET-based human dosimetry of the dimeric $\alpha_v\beta_3$ integrin ligand ^{68}Ga-DOTA-E-[c(RGDfK)]$_2$, a potential tracer for imaging tumor angiogenesis. *J Nucl Med.* 2016;57:404–409.
17. Barlesi F, Scherpereel A, Gorbunova V, et al. Maintenance bevacizumab-pemetrexed after first-line cisplatin-pemetrexed-bevacizumab for advanced nonsquamous nonsmall-cell lung cancer: updated survival analysis of the AVAPERL (MO22089) randomized phase III trial. *Ann Oncol.* 2014;25:1044–1052.
18. Vatsa R, Bhusari P, Kumar S, et al. Integrin $\alpha_v\beta_3$ as a promising target to image neoangiogenesis using in-house generator-produced positron emitter ^{68}Ga-labeled DOTA-arginine-glycine-aspartic acid (RGD) ligand. *Cancer Biother Radiopharm.* 2015;30:217–224.
19. Cardona AF, Rojas L, Wills B, et al. Pemetrexed/carboplatin/bevacizumab followed by maintenance pemetrexed/bevacizumab in Hispanic patients with non-squamous non-small cell lung cancer: outcomes according to thymidylate synthase expression. *PLoS One.* 2016;11:e0154293.
20. Morabito A, Piccirillo MC, Costanzo R, et al. Vandetanib: an overview of its clinical development in NSCLC and other tumors. *Drugs Today (Barc).* 2010;46:683–698.
21. Delmotte P, Martin B, Paesmans M, et al. VEGF and survival of patients with lung cancer: a systematic literature review and meta-analysis [in French]. *Rev Mal Respir.* 2002;19:577–584.
22. Dowlati A, Robertson K, Radivoyevitch T, et al. Novel phase I dose de-escalation design trial to determine the biological modulatory dose of the antiangiogenic agent SU5416. *Clin Cancer Res.* 2005;11:7938–7944.
23. Hanrahan EO, Ryan AJ, Mann H, et al. Baseline vascular endothelial growth factor concentration as a potential predictive marker of benefit from vandetanib in non-small cell lung cancer. *Clin Cancer Res.* 2009;15:3600–3609.
24. Baum RP, Kulkarni HR, Muller D, et al. First-in-human study demonstrating tumor-angiogenesis by PET/CT imaging with ^{68}Ga-NODAGA-THERANOST, a high-affinity peptidomimetic for $\alpha_v\beta_3$ integrin receptor targeting. *Cancer Biother Radiopharm.* 2015;30:152–159.
25. Cai W, Niu G, Chen X. Imaging of integrins as biomarkers for tumor angiogenesis. *Curr Pharm Des.* 2008;14:2943–2973.
26. Haubner R, Wester HJ, Burkhart F, et al. Glycosylated RGD-containing peptides: tracer for tumor targeting and angiogenesis imaging with improved biokinetics. *J Nucl Med.* 2001;42:326–336.
27. Felding-Habermann B, Fransvea E, O'Toole TE, Manzuk L, Faha B, Hensler M. Involvement of tumor cell integrin alpha v beta 3 in hematogenous metastasis of human melanoma cells. *Clin Exp Metastasis.* 2002;19:427–436.
28. Shi J, Jin Z, Liu X, et al. PET imaging of neovascularization with ^{68}Ga-3PRGD2 for assessing tumor early response to Endostar antiangiogenic therapy. *Mol Pharm.* 2014;11:3915–3922.
29. DiCara D, Rapisarda C, Sutcliffe JL. Structure-function analysis of Arg-Gly-Asp helix motifs in αvβ6 integrin ligands. *J Biol Chem.* 2007;282:9657–9665.
30. Eo JS, Jeong JM. Angiogenesis imaging using ^{68}Ga-RGD PET/CT: therapeutic implications. *Semin Nucl Med.* 2016;46:419–427.
31. Kazmierczak PM, Todica A, Gildehaus FJ, et al. ^{68}Ga-TRAP-(RGD)$_3$ hybrid imaging for the *in vivo* monitoring of $\alpha_v\beta_3$-integrin expression as biomarker of anti-angiogenic therapy effects in experimental breast cancer. *PLoS One.* 2016;11:e0168248.
32. Withofs N, Signolle N, Somja J, et al. ^{18}F-FPRGD2 PET/CT imaging of integrin $\alpha_v\beta_3$ in renal carcinomas: correlation with histopathology. *J Nucl Med.* 2015; 56:361–364.
33. Rylova SN, Barnucz E, Fani M, et al. Does imaging $\alpha_v\beta_3$ integrin expression with PET detect changes in angiogenesis during bevacizumab therapy? *J Nucl Med.* 2014;55:1878–1884.
34. Byzova TV, Goldman CK, Pampori N, et al. A mechanism for modulation of cellular responses to VEGF: activation of the integrins. *Mol Cell.* 2000;6:851–860.